case of $f \ll 1$ for the main-resonance mode, the value of ω_d from (54) is ~ 0.67 times as large as that from (53).

The exact solution[24] for the infinite-film problem in circular-cylindrical coordinates for no exchange ($D=0$) is given by (30) with

$$\sin^2\theta_k = k_\rho^2/(k_\rho^2+k_z^2)\,, \tag{55}$$

where k_z is given by (32) (or the corresponding result for odd modes) with k_f replaced by k_ρ. For pinning at the edges of the film ($r_0=0$), the values of k_ρ are given by the roots of the equation

$$J_l(k_\rho r_0)=0\,.$$

Thus, the values of k_ρ are different for modes having different values of azimuthal number l. For $l=0$, this gives the values $k_\rho = 0.76\pi/r_0$, $1.76\pi/r_0$, ... listed in Sec. 5. Considering the other values of l offers an explanation[24] of the observation of Dillon[6] that the first, second, ..., fifth modes in a sample containing a small imperfection on its edge contained one, two, ..., five lines, respectively.

PHYSICAL REVIEW B VOLUME 1, NUMBER 9 1 MAY 1970

Ferromagnetic Resonance in Thin Films. II. Theory of Linewidths

M. SPARKS*
Science Center, North American Rockwell Corporation, Thousand Oaks, California 91360
(Received 28 July 1969)

The ferromagnetic-resonance linewidth ΔH from two-magnon processes in thin films is calculated. The results are quite different from those in spheroidal samples in general, since both the densities of states and the scattering Hamiltonians are different. It is shown that it should be possible to choose the radius and thickness of a ferromagnetic insulator thin film in such a way to make the frequency of the main-resonance mode lie well below the frequencies of all other magnetic modes. The resulting small ΔH's make the films important for studying ferromagnetic-resonance linewidths and afford a useful low-loss system. For scattering centers (such as pits and scratches on the surface of the sample or etch pits extending through the sample thickness) which are smaller than the film thickness, the results are similar to those of Sparks, Loudon, and Kittel (SLK) for a spherical sample. A modification of the SLK result is given which removes the divergence in ΔH at parallel resonance and also makes ΔH go smoothly to zero at perpendicular resonance. For scattering centers which are larger than the film thickness, ΔH has a rather large maximum at an angle approximately one-half way between perpendicular and parallel resonance, in contrast to the small-scattering-center result of a maximum at parallel resonance. In addition to these results for the main-resonance mode, it is shown that the mode-number-n dependence of the two-magnon linewidths of exchange modes (having negligible microwave demagnetization energy) varies in a rather complicated way from $\Delta H \sim n^3$ for small n to $\Delta H \sim n^2$ and $\Delta H \sim n$ for intermediate n to $\Delta H \sim n^0$ for large n.

1. INTRODUCTION

RECENTLY, Mee and co-workers[1] have succeeded in growing single-crystal thin films of yttrium iron garnet (YIG) ranging in thickness from ~ 0.5 to 40 μ. Since bulk films can be ground to a thickness as small as 15 μ, single-crystal YIG films with any thickness greater than ~ 0.5 μ are now available. These films promise to become important ferromagnetic-resonance systems for the following reasons: It is possible to choose the thickness S and the radius R of a film in such a way that there are no magnetic modes degenerate with the main-resonance mode of the film. The resulting small linewidths ΔH should be important for applications requiring low-loss materials, and linewidth mechanisms which were heretofore masked by the large two-magnon process could be investigated in resonance experiments, as discussed elsewhere.[2]

The density of degenerate states can be controlled experimentally over a vast range from zero to very large values. It may be possible to study such interesting effects as mode clamping,[3] comparison of the relaxation frequencies of wave packets and standing waves, linewidths of surface waves on the YIG-substrate interface and on the YIG-air interface, interaction of magnetic and acoustic surface waves, effect of the nonzero relaxation frequencies of the degenerate modes, and comparison of golden-rule relaxation frequencies with normal-mode relaxation frequencies.

The ferromagnetic-resonance linewidth arising from two-magnon scattering in bulk-type samples (e.g., spheroids and thick disks) has been considered by

* Present address: The RAND Corp., Santa Monica, Calif., 90406.

[1] J. E. Mee, J. L. Archer, R. H. Meade, and T. N. Hamilton, Appl. Phys. Letters **10**, 289 (1967); J. E. Mee, IEEE Trans. **MAG-3**, 190 (1967).

[2] M. Sparks, Phys. Rev. Letters **22**, 1310 (1969).

[3] M. Sparks, Quart. Appl. Math (to be published).

several investigators.[4–6] We shall show that the two-magnon linewidth ΔH_2 in thin films is quite different in general from that in bulk-type samples. The first reason for the difference is that the large spacing π/S, where S is the film thickness, between the modes along the z axis in k space for thin films makes the density of degenerate states quite different from that in bulk-type samples in general. Second, for scattering by an imperfection which is large with respect to the film thickness (a large etch pit, for instance), the scattering Hamiltonian is quite different from that in bulk-type samples. The two most striking differences are the possibility of obtaining small ΔH's in thin films, as discussed above, and the different angular dependence of ΔH. (See Figs. 3 and 5 and the related discussion in Sec. 3.) Only the linewidth of the main-resonance mode is considered in the body of the paper. The linewidths of the higher-branch modes are considered briefly in the Appendix. A summary of the theoretical results is given in Sec. 4.

The calculations in the present paper are based on scattering from nonmagnetic voids in the film, and the results are given for the specific case of pits and scratches on the surface of the film. The general results, such as those concerning the range k_c of the scattering in k space for imperfections of a given size R_p, are not restricted to surface pits and scratches. The modifications required for scattering from an arbitrary inhomogeneous H_i are simple. Since the linewidth of the main-resonance mode in a metallic film typically is dominated by eddy-current loss, the present results for the main-resonance mode are more useful in ferromagnetic insulators. The results in the Appendix for the higher-branch exchange modes are valid for insulator and metallic films.

In Paper I[7] of this series, a theory of the frequencies of the ferromagnetic normal modes in films was developed, and in Paper III a theory of surface-spin pinning will be presented. In Paper IV, the effect of an inhomogeneous internal field and saturation magnetization on high-order modes will be considered, and a surface-imperfection source of the inhomogeneities will be investigated. In Paper V, experimental results will be presented and explained in terms of the theories.

2. DISPERSION RELATIONS IN THIN FILMS

In Paper I of this series it was shown that the ordinary spin-wave frequencies

$$\frac{\omega}{|\gamma|}=H_i+Dk^2+\frac{\omega_d}{|\gamma|},\quad \frac{\omega_d}{|\gamma|}=2\pi M_s\sin^2\theta_k, \tag{1a}$$

where γ is the gyromagnetic ratio, H_i is the internal (demagnetized) field, D is the exchange constant, M_s is the saturation magnetization, and θ_k is the angle between the wave vector $\mathbf{k}$ and $\mathbf{H}_i$ (along the z axis), can be used for the ferromagnetic-normal-mode frequencies in thin films with finite radius R if the discrete values of k_x, k_y, and k_z are chosen properly. In (1a) the circular-precession approximation[8] has been made. For spin waves at 9.7 GHz in YIG this gives an error ranging from 0 to 6%, depending on the values of Dk^2 and $\sin^2\theta_k$.[8] At lower frequencies (1a) should still be a good approximation for the small-k modes of interest if $2\pi M_s$ is replaced by $[(H_i)(H_i+4\pi M_s)]^{1/2}-H_i$, which is the width of the magnon manifold at $k=0$. Of course, the full dispersion relation[7]

$$\omega/|\gamma|=[(H_i+Dk^2)(H_i+Dk^2+4\pi M_s\sin^2\theta_k)]^{1/2} \tag{1b}$$

could be used if better than order-of-magnitude accuracy in the linewidths were required, but the algebra becomes more involved.

In considering the distribution of modes in $\mathbf{k}$ space we use a square film of dimensions $L\times L\times S$ with zero boundary conditions at $x=\pm\frac{1}{2}L$ and at $y=\pm\frac{1}{2}L$. This is similar to the familiar approximation of using periodic boundary conditions on the edges of a square box to obtain plane waves. The appropriate values of k_x, k_y, and k_z for perpendicular resonance[9] are[7]

$$\begin{aligned} &k_x=\frac{n_x\pi}{L},\quad k_y=\frac{n_y\pi}{L}, && n_x, n_y=1, 2, 3\ldots \\ &k_z=\left(\frac{2k_f}{S}\right)^{1/2},\ \frac{\pi}{S},\ \frac{2\pi}{S},\ldots, && k_f^2\equiv k_x^2+k_y^2 \end{aligned} \tag{2}$$

for $k_fS\gtrsim 1$. These values are intuititively plausible: For an infinite film k_x and k_y are continuous and k_z has discrete values (for given values of k_x and k_y). The discrete values of k_x and k_y in (2) for the finite film are for pinning[10] of the microwave magnetization at the small edges of the film (at x, $y=\pm\frac{1}{2}L$), and the discrete values of k_z are those for an infinite film having the values of k_x and k_y given in (2).

Combining (1a) and (2) gives

$$\omega_d\cong\pi|\gamma|M_sk_fS \qquad \text{for } k_z=\left(\frac{2}{\pi^2}k_fS\right)^{1/2}\frac{\pi}{S} \tag{3a}$$

$$\omega_d\cong\frac{2}{\pi}|\gamma|M_s\left(\frac{k_fS}{n_z}\right)^2 \qquad \text{for } k_z=\frac{n_z\pi}{S};\ n_z=1, 2, \ldots \tag{3b}$$

[4] A. M. Clogston, H. Suhl, L. R. Walker, and P. W. Anderson, J. Phys. Chem. Solids 1, 129 (1956).

[5] M. Sparks, R. Loudon, and C. Kittel, Phys. Rev. 122, 791 (1961).

[6] P. E. Seiden and M. Sparks, Phys. Rev. 137, A1278 (1965).

[7] M. Sparks, preceding paper, Phys. Rev. B 1, 3831 (1970).

[8] M. Sparks, *Ferromagnetic Relaxation Theory* (McGraw-Hill Book Co., New York, 1964), Sec. 3.3, p. 69.

[9] Perpendicular (or parallel) resonance indicates that the applied field $\mathbf{H}_{\text{app}}$ is perpendicular (or parallel) to the plane of the film.

[10] The surface spins are said to be *pinned* (or *unpinned*) if the microwave magnetization $\mathbf{m}$ is zero (or the normal derivative of $\mathbf{m}$ is zero) at the surface.

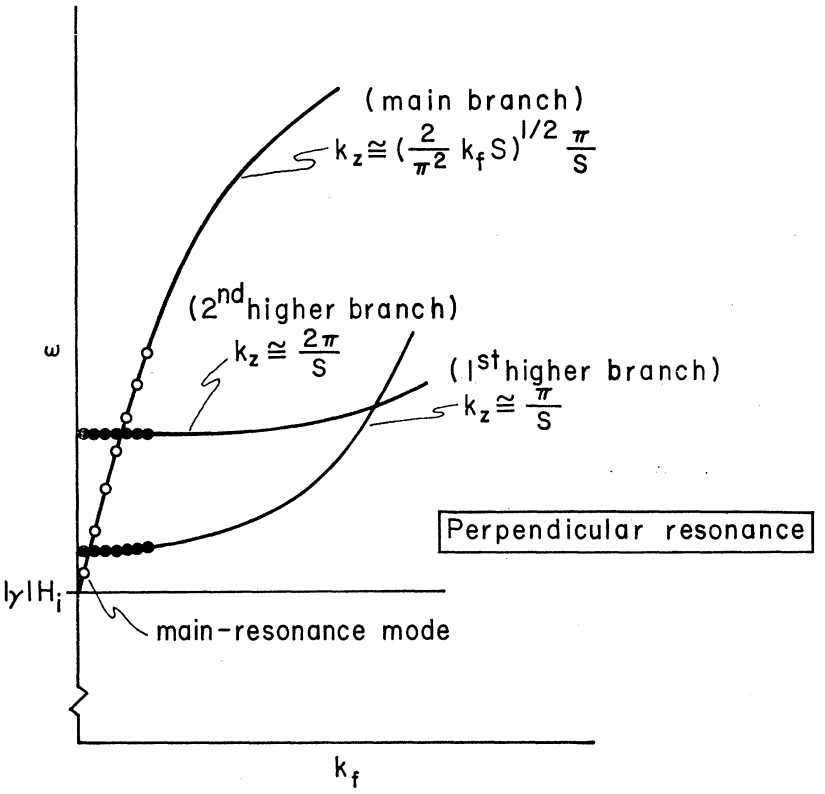

FIG. 1. Dispersion relations for a thin film showing the main-branch modes (open circles) and the higher-branch modes (solid circles).

for the case of perpendicular resonance with $k_f S \lesssim 1$, where $\mathbf{k}_f$ is the wave vector in the plane of the film. The result corresponding to (3a) for an arbitrary value of the angle θ_m between $\mathbf{H}_i$ and the normal to the plane of the film ($\theta_m = 0$ in perpendicular resonance) is[7]

$$\omega_d/|\gamma| = 2\pi M_s \sin^2\theta_m + \pi M_s k_f S(\cos^2\theta_m - \cos^2\phi \sin^2\theta_m), \quad (4)$$

where $\phi = \tan^{-1}(k_y/k_x)$.

In bulk-type samples, ω typically is considered as a function of k with $\sin^2\theta_k$ as a parameter. In thin films the large spacing π/S of the modes along the z axis in k space makes it convenient to consider the frequency ω as a function of k_x and k_y, with k_z as a parameter labeling different *branches*. This is illustrated in Fig. 1, which is a schematic representation of the dispersion relations (1a) for perpendicular resonance. The branch having the lowest value of k_z (open circles in Fig. 1) will be called the *main branch*, and those having larger values of k_z (solid points in Fig. 1) will be called the *higher branches*. The main-branch mode having the smallest value of k_f will be called the *main-resonance mode*.

The effect of Portis-type pinning[10a] on the linewidths will not be considered in detail. The scattering out of low-order Portis modes by surface imperfections could be smaller than the corresponding results for sine-wave modes because the amplitudes of the Portis modes are smaller near the surfaces of the sample where the scattering fields are largest. The nonzero slopes[7] of the low-order modes at $k_f = 0$ may reduce the value of ΔH by reducing the density of degenerate states.

3. CALCULATION OF TWO-MAGNON LINEWIDTH

We consider the ferromagnetic-resonance linewidth for two-magnon scattering induced by large scale imperfections [say between $(100\ \text{Å})^3$ and 10^{-1} times the sample volume V] such as pits and scratches on the sample surface, etch pits, voids, inclusions of materials of different saturation magnetization, volumes of different crystallographic orientations, inhomogeneous strain, inhomogeneous saturation magnetization, etc. As a model for the imperfection we consider a small pore of nonmagnetic material of volume $V_p \ll V$ introduced into the sample. The resulting two-magnon linewidth depends on the size and shape of the pore and on its position in the sample. Two cases are considered: scattering by small pits (diameter $2R_p \ll S$) on the sample surface and scattering by large etch pits (diameter $2R_p \gg S$) which extends across the thickness of the sample.

Linewidth for small pits ($2R_p \ll S$). First consider the scattering out of the main-resonance mode by a small spherical pore far away from the sample surface. The

[10a] A. M. Portis, Appl. Phys. Letters 2, 69 (1963).

magnetization $\mathbf{M}$ can be approximated by

$$\mathbf{M}=M_s\hat{z}+\mathbf{m},$$

where M_s is the (constant) saturation magnetization and the transverse microwave magnetization $\mathbf{m}$ (where $\mathbf{m}\cdot\hat{z}=0$) is a function of position $\mathbf{r}$, which can be approximated by a standing sine wave. The Hamiltonian for scattering out of the Kittel mode (plane wave with $\mathbf{k}=0$) into other plane-wave modes $\mathbf{k}$ is[5,6,11]

$$\mathcal{H}=\sum_k \hbar F_k(b_r^\dagger b_k+b_k^\dagger b_r),$$

where

$$F_k^2=(5.6/16)(4\pi\gamma M_s)^2(V_p/V)^2A_kC_k \tag{5}$$

with the angle factor[11] A_k and cutoff factor C_k defined as

$$\begin{aligned}A_k&\equiv[(3\cos^2\theta_k-1)^2+1.6]/5.6,\\ C_k&\equiv[3j_1(kR_p)/kR_p]^2.\end{aligned} \tag{6}$$

The $b^\dagger$ and b are creation and annihilation operators, r denotes the main-resonance mode (Kittel mode for plane waves) and $j_1(x)\equiv(\sin x-x\cos x)/x^2$. For small pits, the microwave magnetization of the main-resonance mode in the finite films is constant in the vicinity of a pit, and the analysis leading to (5) is unchanged for standing waves apart from numerical factors arising from the integral in $\mathcal{H}=-\frac{1}{2}\int d\mathbf{r}\mathbf{h}\cdot\mathbf{m}$. Replacing the plane-wave factor $\exp(i\mathbf{k}\cdot\mathbf{r})$ in Eq. (3.69) of Ref. 8 by the normalized standing-wave factor $(\sqrt{2}\cos k_x x)(\sqrt{2}\cos k_y y)$ gives

$$m^+\equiv m_x+im_y=\left(\frac{2|\gamma|\hbar M_s}{V}\right)^{1/2}\sum_k 2\cos k_x x\cos k_y y\, b_k. \tag{7}$$

The plane-wave value of F_k^2 in (5) must be multiplied by $(2\sqrt{2}/\pi)^8$ [where $(1/\pi)\int_0^\pi dx\sqrt{2}\cos x=2\sqrt{2}/\pi$] to account for the average over the standing waves along the x and y axis of modes $\mathbf{k}$ and r.

Just as in the Sparks-London-Kittel calculation,[5] we must take into account the fact that there are hemispherical pits on the surface of the sample rather than spherical pits in an infinite volume. It is plausible that the scattering Hamiltonian should be reduced by a factor of $\frac{1}{2}$ to account for the reduction in the effective magnetic moment of the scatterer and a factor of $\frac{1}{2}$ to account for integrating over a semi-infinite half-space rather than over an infinite volume. Thus F_k^2 in (5) must be multiplied by $(2\sqrt{2}/\pi)^8(\frac{1}{2})^4=(2/\pi)^8$.

The Born-approximation result for the linewidth for scattering from a single spherical pit in the center of a large sample is

$$\begin{aligned}\Delta H_{\text{one pit}}&=\frac{2}{|\gamma|}\sum_k|F_k|^2\frac{G_k}{\frac{1}{2}|\gamma|\Delta H_k},\\ G_k&\equiv\frac{(\frac{1}{2}\gamma\Delta H_k)^2}{(\omega_r-\omega_k)^2+(\frac{1}{2}\gamma\Delta H_k)^2},\end{aligned} \tag{8}$$

[11] M. Sparks, Ref. 8. See Eq. (5.3) and p. 86.

where $\frac{1}{2}|\gamma|\Delta H_k$ is the relaxation frequency (assumed to be independent of $\mathbf{k}$ for simplicity) of the modes coupled to the relaxing mode r, ω_r is the frequency of mode r, and ω_k are the frequencies of the coupled modes $\mathbf{k}$.

In the line-shape factor G_k we have not taken the usual δ-function limit

$$\lim_{\frac{1}{2}|\gamma|\Delta H_k\to 0}\frac{(\frac{1}{2}|\gamma|\Delta H_k)}{(\omega_r-\omega_k)^2+(\frac{1}{2}\gamma\Delta H_k)^2}=\pi\delta(\omega_r-\omega_k), \tag{9}$$

since off-resonance scattering will be considered. Multiplying $\Delta H_{\text{one pit}}$ in (8) by the factor $(2/\pi)^8$ from above and by the number of surface pits $2\pi R^2/(2R_p)^2$ (assuming square-lattice packing and independent scattering by the individual pits) and using (5) gives

$$\begin{aligned}\Delta H_{\text{sml pits}}&=H_1\Sigma_k,\quad \Sigma_k=\sum_k A_kC_kG_k,\\ H_1&=\frac{5.6}{9}\left(\frac{2}{\pi}\right)^7\frac{(4\pi M_s)^2}{\Delta H_k}\frac{(2R_p)^4}{(2R)^2S^2},\end{aligned} \tag{10}$$

where A_k, C_k, and G_k are defined in (6) and (8). A convenient form of H_1 is

$$H_1=\left(\frac{4\pi M_s}{1750}\right)^2\left(\frac{0.2}{\Delta H_k}\right)\left(\frac{2R_p}{0.25\mu}\right)^4\left(\frac{20\text{ mil}}{2R}\right)^2\left(\frac{1\mu}{S}\right)^2\times 6.1\text{ mOe} \tag{11}$$

where $20\text{ mil}=5\times 10^2\mu$.

Evaluation of Σ_k for small pits. The scattering Hamiltonian for *small* pits couples the main-resonance mode strongly to both the higher-branch and main-branch modes, as seen in (5). Because of this and the fact that the sum over $\mathbf{k}$ in (8) contains many large terms from many different branches (except at perpendicular resonance in very thin films—which is discussed separately in the following subsection), the δ-function approximation (9) can be used for the line-shape factor G_k in (8) and (10). Also, the dispersion relation (1a) can be used with $\sin^2\theta_k$ considered as a continuous parameter for this case. That is, the dispersion relation for the coupled modes $\mathbf{k}$ is essentially the same as for ordinary magons.

Approximating the sum in (10) by an integral, making the δ-function approximation (9), and using

$$\delta(\omega_k-\omega_r)=\frac{1}{4\pi|\gamma|M_su_k}[\delta(u-u_k)+\delta(u+u_k)], \tag{12}$$

where $u\equiv\cos\theta_k$ and

$$u_k^2=\frac{H_i+Dk^2+2\pi M_s-(\omega_r/|\gamma|)}{2\pi M_s}\equiv\frac{\Lambda}{2\pi}k^2+u_0^2, \tag{13}$$

$$u_0^2\equiv u_k^2|_{k=0},\quad \Lambda\equiv D/M_s$$

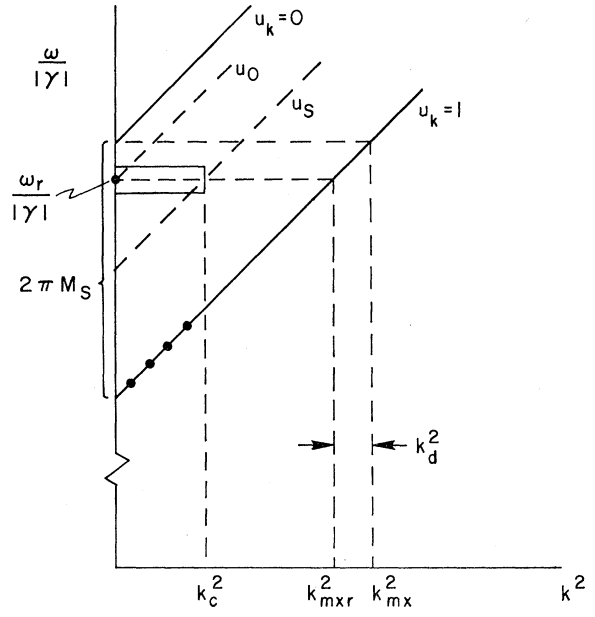

FIG. 2. Usual magnon dispersion relation, shown to illustrate the meaning of u_0, u_s, k_d^2, k_c^2, $k_{\max r}^2$, and $k_{\max}^2$. In this figure, $k_c^2<k_{\max r}^2$; thus $k_s=k_c$. The dots are discussed in the Appendix.

gives

$$\Sigma_k=\frac{V}{\pi^3}\frac{\frac{1}{2}|\gamma|\Delta H_k(\frac{1}{2}\pi)\pi}{4\pi|\gamma|M_s}\int_0^\infty dk\,k^2\frac{C_kA_k}{u_k}\times\int_0^1 du\,\delta(u-u_k). \quad (14)$$

The value of the u integral is 1 for $0<u_k<1$ and 0 otherwise. For $H_i\leqq\omega_r/|\gamma|\leqq H_i+2\pi M_s$, $u_k<1$ gives $k<k_{\max r}$, where

$$k_{\max r}\equiv\left[\left(\frac{2\pi}{\Lambda}\right)(1-u_0^2)\right]^{1/2}$$

is the maximum value of k for modes degenerate with the main-resonance mode r. (See Fig. 2.) Thus, the upper limit of ∞ in the k integral in (14) is replaced by $k_{\max r}$. The function $C_k\equiv[3j_1(kR_p)/kR_p]^2$ can be approximated by the unit-step function

$$C_k\cong\theta(k_c-k),\quad k_c\cong(9/2\pi^2)^{1/3}\pi/R_p. \quad (15)$$

The cutoff value of $k_c=(9/2\pi)^{1/3}(\pi/R_p)$ was chosen to make

$$\int_0^{k_c}dk\,k^2=\int_0^\infty dk\,k^2C_k=\frac{3\pi}{2R_p{}^3};$$

with these two results, (14) gives

$$\Sigma_k=\frac{V}{4\pi}\frac{\Delta H_k}{4\pi M_s}\int_0^{k_s}dk\frac{k^2A_k}{[(\Lambda/2\pi)k^2+u_0^2]^{1/2}}, \quad (16)$$

where k_s is k_c or $k_{\max r}$, whichever is smaller. Since A_k is not a strong function of k and k^2 weights the large values of k, A_k can be evaluated at $k=k_s$ and taken outside the integral. Evaluating the integral in (16) and using (10) then gives

$$\Delta H=\frac{5.6\sqrt{(2\pi)}}{288}\left(\frac{2}{\pi}\right)^7 4\pi M_s\frac{(3u_s^2-1)^2+1.6}{5.6}\frac{(2R_p)^4}{S\sqrt{\Lambda}}\times\left[k_s(k_s^2+k_d^2)^{1/2}-k_d^2\ln\frac{k_s+(k_s^2+k_d^2)^{1/2}}{k_d}\right], \quad (17)$$

where

$$k_d^2\equiv 2\pi u_0^2/\Lambda=k_{\max}^2-k_{\max r}^2,$$
$$k_{\max}\equiv(2\pi M_s/D)^{1/2}=(2\pi/\Lambda)^{1/2},$$

and $u_s\equiv u_k|_{k=k_s}$. (See Fig. 2.)

Several limiting cases of (17) are of interest. If the scattering centers are not too small (i.e., if $k_c\ll k_{\max}$), then $k_s=k_c<k_{\max r}$ is satisfied everywhere in the manifold except very near the bottom. The bracket factor in (17) has the limiting values of $2k_c^3/3k_d$ for $k_d^2\gg k_c^2$ and k_c^2 for $k_d^2\ll k_c^2$, and (17) reduces to

$$\Delta H_{\text{sml pits}}=\frac{5.6}{6}\left(\frac{2}{\pi}\right)^6 4\pi M_s\frac{(3u_s^2-1)^2+1.6}{5.6u_0}\frac{2R_p}{S}B$$
$$=\left(\frac{4\pi M_s}{1750}\right)\left(\frac{2R_p}{0.25\mu}\right)\left(\frac{1\mu}{S}\right)\times\frac{(3u_s^2-1)^2+1.6}{5.6u_0}B\times 27.2\text{ Oe},$$

where

$$B=1,\quad \text{for } k_d^2\gg k_c^2$$
$$=\frac{3}{2}\frac{1}{k_c}\left(\frac{2\pi}{\Lambda}\right)^{1/2}u_0,\quad \text{for } k_c^2\gg k_d^2 \quad (18a)$$

$$k_c=\left(\frac{9}{2\pi^2}\right)^{1/3}\frac{\pi}{R_p}=0.769\frac{\pi}{R_p},$$

$$k_d=\left(\frac{2\pi}{\Lambda}\right)^{1/2}u_0=4.4u_0\times 10^5,$$

$$k_{\max}=(2\pi/\Lambda)^{1/2},\quad k_{\max r}\equiv[(2\pi/\Lambda)(1-u_0^2)]^{1/2},$$

$$k_s=\text{lesser of } (k_c,k_{\max r}),$$

for this case of $k_c\ll k_{\max}$. The top value of $B=1$ is valid everywhere in the manifold except near the top or bottom, and the bottom value of B is valid near the top of the manifold. Near the bottom of the manifold, the inequality $k_c<k_{\max r}$ is not satisfied since $k_{\max r}\to 0$ at the bottom. This makes $H\sim k_{\max r}{}^3$ near the bottom of the manifold, as will be shown in (18b).

For $k_c \ll k_{\max}$ and $k_d^2 \gg k_c^2$, the present result (18a) with $B=1$ reduces to that of Sparks, Loudon, and Kittel[5] with the Seiden and Sparks angle factor[6] included and the appropriate change for the number of surface pits on a thin film rather than a spherical sample. The present result (18a) is not limited to the case of relatively large scattering centers ($R_p \gtrsim 1\,\mu$ in parallel resonance, and even larger in perpendicular resonance), as were the results of Sparks, Loudon, and Kittel.

Note that ΔH in (18a) remains finite at $u_0=0$ (parallel resonance in an infinite film) because u_0 in B cancels $1/u_0$ in the coefficient of B in (18a). Thus, the new result (18a) removes the troublesome divergence in parallel resonance without having to invoke arguments about the finite size of ΔH_k.[6]

The result (16) is valid for ω_r above the top of the manifold, i.e., for $\omega_r > |\gamma|(H_i+2\pi M_s)$, in which case k_d^2 is negative, if the lower limit of zero in the integral is replaced by $|k_d|$. For $|k_d| > k_c$ the value of the integral is to be taken as zero. For the present case of fairly large scatters, i.e., $k_c^2 \ll k_{\max}^2$, the value of $|k_d|$ is equal to k_c for ω_r slightly above the top of the manifold, causing ΔH to drop to zero fairly sharply at the top of the manifold.

The value of $\Delta H_{\text{sml pits}}$ from (18a) is sketched as a function of the angle θ_m between $\mathbf{H}_i$ and the film normal in Fig. 3. The functional form of the angle factor $[(3u_s^2-1)^2+1.6]/u_0$ in (18a) is somewhat arbitrary.[6,8] and the value of ΔH at the minimum in Fig. 3 is rather sensitive to this factor, but the general features of the figure are otherwise relatively insensitive to the details of the model.

Next consider the limiting case of very small scattering centers, i.e., $k_c > k_{\max r}$, for which the relaxing mode scatters into all degenerate modes. In this case $k_s = k_{\max r}$ and $k_s^2+k_d^2 = k_{\max}^2 = 2\pi/\Lambda$ in the bracket factor in (17). Expanding the bracket factor gives $k_{\max r}^3(\Lambda/2\pi)^{1/2}$ for $Dk_{\max r}^2 \ll 2\pi M_s$ (i.e., near the bottom of the manifold) and $k_{\max r}(2\pi/\Lambda)^{1/2}$ for $|k_d^2| \ll k_{\max}^2$ (i.e., near the top of the manifold, either above or below), and (17) reduces to

$$\Delta H_{\text{vy sml pits}} = \frac{5.6}{288}\left(\frac{2}{\pi}\right)^7 4\pi M_s \times \frac{(3u_s^2-1)^2+1.6}{5.6}\,\frac{(2R_p)^4}{S}B_s, \quad (18b)$$

where

$$B_s = k_{\max r}^3, \quad \text{for} \quad Dk_{\max r}^2 \ll 2\pi M_s$$
$$= (2\pi/\Lambda)k_{\max r}, \quad \text{for} \quad |k_d^2| \ll k_{\max}^2$$

for this "equal-scattering" case of $k_c > k_{\max r}$. The top value of B_s is valid near the bottom of the manifold and the bottom value is valid near the top of the manifold. The value of $k_{\max r}$ increases as ω_r increases,

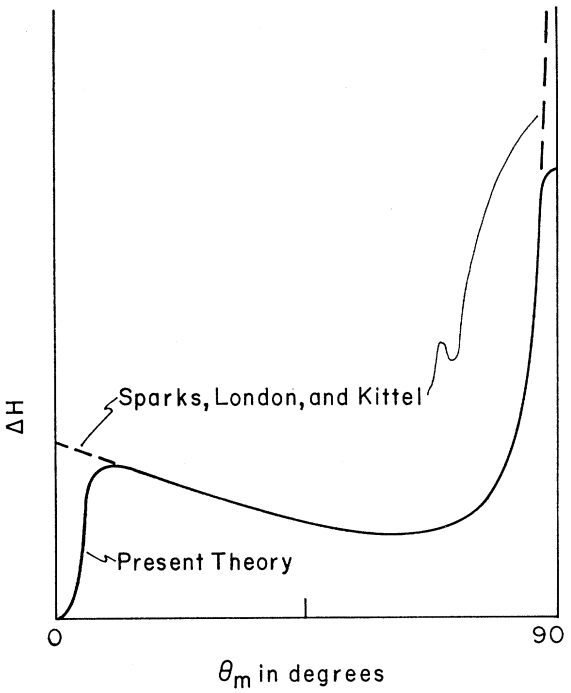

FIG. 3. Angular dependence of the two-magnon ΔH for scattering centers smaller than the film thickness. The results are the same as those for bulk-type samples except for the different number of scattering centers on the surfaces of the samples. The previous results of Sparks, Loudon, and Kittel are shown as a dashed curve.

and $k_{\max r} < k_c$ is no longer satisfied for sufficiently large values of ω_r. At this point ΔH drops below the value given in (18b).

The linewidth in (18a) goes smoothly to zero at the bottom of the manifold ($u_0 \to 1$). Thus ΔH will be small in thin films in perpendicular resonance since u_0 is small. For example, for $2R_p=0.25\,\mu$, $S=1\,\mu$, and the main-resonance mode 6 Oe above the bottom of the spin-wave manifold in YIG, (18a) gives $\Delta H=1.5$ Oe, which is to be compared with $\Delta H=85$ Oe for the corresponding conditions ($\delta H=6$ Oe) in parallel resonance. The results (18a) should be valid for parallel resonance in general and for values of θ_m not too near zero (so that there are many higher branches with $\omega < \omega_r$). We shall now show that in very thin films in perpendicular resonance ΔH will be even smaller than the value given by (18a).

$\Delta H_\perp$ in very thin films. By a very thin film we mean that the modes in the first higher branch in perpendicular resonance have higher frequencies than that of the main-resonance mode. In this case there are no modes degenerate with the main-resonance mode. If the aspect ratio $2R/S$ is sufficiently small, the other modes of the main branch are resolved from the main-resonance mode, and scattering into all modes is small.

We now estimate the value of ΔH from off-resonance scattering of the main-resonance mode into the higher

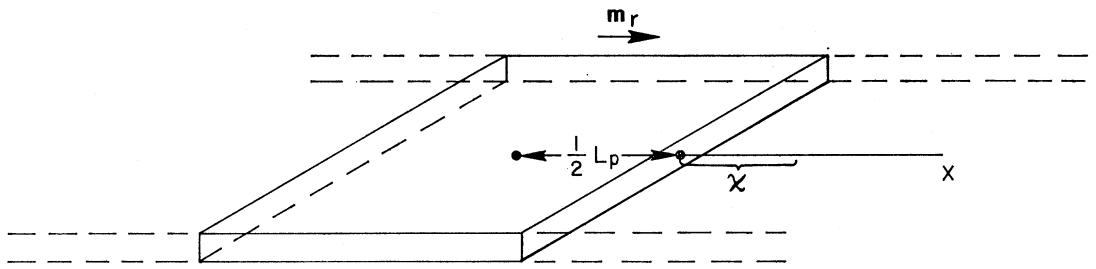

FIG. 4. Geometry of the model of an imperfection used in calculating the linewidth for scattering by large imperfections.

branches. Note that the δ-function approximation (9) gives $\Delta H=0$ since there are no degenerate modes. From (10) with $(\omega_r-\omega_k)^2\gg(\frac{1}{2}\gamma\Delta H_k)^2$ we find

$$\Sigma_k=\frac{L^2}{\pi^2}(\tfrac{1}{2}\gamma\Delta H_k)^2\frac{\pi}{2}\sum_{k_z}\int_0^\infty dk_f\, k_f\frac{1}{(\omega_r-\omega_k)^2}, \quad (19)$$

where the sum over k_x and k_y has been replaced by the integral over k_f. From (3) we find

$$\omega_r-\omega_k=|\gamma|\,\delta H_{n_z}+(2/\pi)|\gamma|M_s(k_fS/n_z)^2,$$

where the spacing δH_{n_z} between the main-resonance mode and the $k_f=0$ limit of the exchange mode with $k_z=\pi n_z/S$ is

$$\delta H_{n_z}\cong D(\pi n_z/S)^2.$$

Using these results and evaluating the integral in (19) gives

$$\Sigma_k\cong\sum_{k_z}\frac{1}{32}\frac{(\Delta H_k)^2}{4\pi M_s}\frac{(2R)^2}{D}. \quad (20)$$

Since the summand is independent of k_z, the value of the sum is the summand times the number of terms in the sum. The number of modes with $k_z<k_c$ is $(9\pi/2)^{1/3}(2/\pi)(S/2R_p)$, which gives

$$\Sigma_k=\frac{1}{16}\left(\frac{9}{2\pi^2}\right)^{1/3}\frac{(\Delta H_k)^2}{4\pi M_s}\frac{(2R)^2S}{D(2R_p)}$$
$$=\left(\frac{\Delta H_k}{0.2}\right)^2\left(\frac{1750}{4\pi M_s}\right)\left(\frac{4.5\times10^{-9}\text{ Oe cm}^2}{D}\right)$$
$$\times\left(\frac{2R}{20\text{ mil}}\right)^2\left(\frac{S}{1\mu}\right)\left(\frac{0.25\mu}{2R_p}\right)2.5. \quad (21)$$

From (21) and (10)

$$\Delta H=\left(\frac{\Delta H_k}{0.2}\right)\left(\frac{4\pi M_s}{1750}\right)\left(\frac{2R_p}{0.25\mu}\right)^3$$
$$\times\left(\frac{4.5\times10^{-9}\text{ Oe cm}^2}{D}\right)\left(\frac{1\mu}{S}\right)\times15.4\text{ mOe}. \quad (22)$$

This value of ~15 mOe is much smaller than the corresponding value of 1.5 Oe obtained formally from (18a). It is easy to show that the contribution to ΔH from scattering by pits with $2R_p\gg S$ in very thin films in perpendicular resonance is also very small.

Linewidth for large pits ($2R_p\gtrsim S$). We first find the Hamiltonian for scattering out of the main-resonance mode into modes with $k_z=0$ and $k_f\equiv(k_x^2+k_y^2)\lesssim\pi/R_p$ (so that the magnetization of both modes is essentially constant over the pit). Consider the scattering by a pit which extends across the thickness of the film, such as a pit etched all the way through the film to the substrate. As a model we consider a square void of sides L_p (and thickness S). The difference between this square void and observed etch pits, which are typically nearly circular, should not be important in an order-of-magnitude calculation.

The scattering Hamiltonian is

$$\mathcal{H}=-\frac{1}{2}\int d\mathbf{r}\,\mathbf{h}_d\cdot\mathbf{m}. \quad (23)$$

Expanding $\mathbf{m}$ and the demagnetization field $\mathbf{h}_d$ in the normal modes of the film gives products of creation and annihilation operators of the relaxing mode r and the remaining modes k. It is easy to show that[12,13]

$$\int d\mathbf{r}\,\mathbf{h}_r\cdot\mathbf{m}_k=\int d\mathbf{r}\,\mathbf{h}_k\cdot\mathbf{m}_r,$$

where $\mathbf{m}_k$ (or $\mathbf{m}_r$) is the magnetization of mode $\mathbf{k}$ (or mode r) and $\mathbf{h}_k$ (or $\mathbf{h}_r$) is the demagnetization field from $\mathbf{m}_k$ (or $\mathbf{m}_r$). Thus the term in (23) which couples $\mathbf{k}$ to r can be written as

$$\mathcal{H}=-\int d\mathbf{r}\,\mathbf{h}_r\cdot\mathbf{m}_k, \quad (24)$$

and we must calculate only $\mathbf{h}_r$, and not $\mathbf{h}_k$. The solution to the usual equations

$$\nabla\cdot\mathbf{b}_r=\nabla\cdot(\mathbf{h}_r+4\pi\mathbf{m}_r)=0,\quad \nabla\times\mathbf{h}_r=0$$

[12] C. Warren Haas and Herbert B. Callen, in *Magnetism*, edited by G. T. Rado and H. Suhl (Academic, New York, 1963), Vol. 1.

[13] Jay P. Sage, Phys. Rev. **185**, 859 (1969).

is well known:

$$\mathbf{h}_r=\nabla\psi,\quad \psi(\mathbf{r})=\int d\mathbf{r}'\frac{\nabla'\cdot\mathbf{m}_r(\mathbf{r}')}{|\mathbf{r}'-\mathbf{r}|},\tag{25}$$

where the integral extends over all of space.

First consider the contribution h_+ to the component h_x of $\mathbf{h}_r$ (see Fig. 4) from the δ function in $\nabla\cdot\mathbf{m}_r$ at $\chi=0$ (i.e., at $x=+\frac{1}{2}L_p$), where χ is shown in Fig. 4. From (25),

$$h_+=-\int d\mathbf{r}'\chi\frac{\nabla'\cdot\mathbf{m}_r(\mathbf{r}')}{(\chi^2+z'^2+y'^2)^{3/2}}.\tag{26}$$

Since m_r is constant in the region near the pit, (26) gives

$$h_+=-2m_{rx}\chi\int_{-S/2}^{S/2}dz'\frac{1}{\chi^2+z'^2}\frac{\frac{1}{2}L_p}{[\chi^2+(\frac{1}{2}L_p)^2+z'^2]^{1/2}}.$$

With $\frac{1}{2}L_p\gg\frac{1}{2}S$, z'^2 can be neglected in the square root, giving

$$h_+=-\frac{2m_{rx}L_p}{[\chi^2+(\frac{1}{2}L_p)^2]^{1/2}}\tan^{-1}\frac{S}{2\chi}.\tag{27}$$

We can approximate (27) by

$$\begin{aligned}h_+&\cong-2\pi m_{rx},\quad &&\text{for } 0\leqq\chi\leqq\tfrac{1}{2}S\\&\cong-2m_{rx}\frac{S}{\chi},\quad &&\text{for } \tfrac{1}{2}S\leqq\chi\leqq\tfrac{1}{2}L_p\\&\cong-m_{rx}\frac{L_pS}{\chi^2},\quad &&\text{for } \tfrac{1}{2}L_p\leqq\chi.\end{aligned}\tag{28}$$

The contribution h_- from the surface at $x=-\frac{1}{2}L_p$ is obtained from (28) by multiplying by -1 and replacing χ by $\chi+L_p$. It is easy to show that h_- is negligible for $\chi\gtrsim\frac{1}{4}L_p$. Thus $h_x=h_++h_-$ can be approximated by

$$\begin{aligned}h_x&\cong-2\pi m_{rx},\quad &&\text{for } 0\leqq\chi\leqq\tfrac{1}{2}S\\&\cong-2m_{rx}\frac{S}{\chi},\quad &&\text{for } \tfrac{1}{2}S\leqq\chi\leqq\tfrac{1}{4}L_p.\end{aligned}\tag{29}$$

From (29) and (24) it is not difficult to show that the contribution $\mathcal{H}_<$ to $\mathcal{H}$ from the region $\rho\equiv(x^2+y^2)^{1/2}<\frac{1}{2}L_p$ is approximately

$$\mathcal{H}_<\cong2\pi m_r(p)m_k(p)S^2L_p\left(1+\frac{2}{\pi}\ln\frac{L_p}{2S}\right),\tag{30}$$

where $m_r(p)$ and $m_k(p)$ are the values of m_{rx} and m_{kx} at the pit.

We estimate the contribution $\mathcal{H}_>$ to $\mathcal{H}$ from the region $\rho>\frac{1}{2}L_p$ by using a circular pit of radius R_p. It is easy to show that for $\rho\gg R_p$

$$h_x\cong m_r(p)(V_p/\rho^3)(1-3\cos^2\phi_x),$$

where $\phi_x\equiv\tan^{-1}(y/x)$. Thus

$$\mathcal{H}_>\cong m_r(p)m_x(p)S\int_0^{2\pi}d\phi_x\int_{R_p}^{\infty}d\rho\,\rho\frac{V_p}{\rho^3}(3\cos^2\phi_x-1)$$
$$=\pi^2m_r(p)m_k(p)S^2R_p^2.\tag{31}$$

Adding (30) and (31) and setting $L_p^2=\pi R_p^2$ gives

$$\mathcal{H}=2\pi^{3/2}m_r(p)m_k(p)S^2R_p\times\left(1+\frac{\sqrt{\pi}}{2}+\frac{2}{\pi}\ln\frac{(2\sqrt{\pi})R_p}{4S}\right).\tag{32}$$

The x components $m_r(p)$ and $m_k(p)$ are equal to $m_r(p)=\frac{1}{2}[m_r^+(p)+m_r^-(p)]$ and the corresponding expression with r replaced by k, where $m^\pm=m_x\pm im_y$.

The coupling (from mode r with $k_z=0$ into mode $\mathbf{k}$ with $k_z=0$) is reduced when $k_x\lesssim\pi/R_p$ and $k_y\lesssim\pi/R_p$ since the positive and negative surface poles for $\lambda\lesssim R_p$ make the demagnetization field small. Thus, we multiply $\mathcal{H}$ in (32) by the product $\theta(\pi/R_p-k_y)\theta(\pi/R_p-k_x)$ of unit-step functions. This cutoff factor is analogous to $C_k\cong\theta(k_c-k)$ in (15) and (6).

Using these three results and the fact that $m_r(p)\sim\sqrt{2}\cos(\pi x/L)\sqrt{2}\cos(\pi y/L)=2$ at $x=y=0$ and introducing a factor of $(2\sqrt{2}/\pi)^2$ in $\mathcal{H}$ for the average of $|m_k(p)|$ over k_x and k_y gives

$$\mathcal{H}=\sum_k\hbar F_k(b_r^\dagger b_k+b_k^\dagger b_r),$$

where

$$(F_{k_x,k_y,0})^2=2\left(\frac{2}{\pi}\right)^5\left(1+\frac{\sqrt{\pi}}{2}+\frac{2}{\pi}\ln\frac{(2\sqrt{\pi})R_p}{4S}\right)^2\times(4\pi\gamma M_s)^2\frac{(2R_p)^2S^2}{(2R)^4}\left(\frac{m_r(p)}{m_r(0)}\right)^2.\tag{33}$$

Here $m_r(0)$ is the maximum value of $m_r(\mathbf{r})$ (at $\mathbf{r}=0$).

For the case of $L_p=S$, replacing the integral over y' and z' in (26) by $2\pi\int d\rho\,\rho$ and repeating the analysis above gives

$$\mathcal{H}=2m_r(p)m_k(p)S^3.\tag{34}$$

For a sample containing $N_{p\text{its}}$ pits, we assume independent scattering by the individual pits. In general, both R_p and $m_r(p)$ are different for the different pits, and the value of ΔH for one pit is simply summed over all pits. For simplicity, we assume pits of equal radii R_p, and write the sum over $m_r(p)$ as $\bar{m}_rN_{p\text{its}}$, where $\bar{m}_r$ is the average of $m_r(p)$ over all pits. Then, from (8) and (33) we obtain

$$\Delta H=H_1\Sigma_k,\quad \Sigma_k=\sum_{k_x,k_y<\pi/R_p}G_k,\tag{35}$$

$$H_1=\frac{1}{\pi}\left(\frac{4}{\pi}\right)^4\frac{(4\pi M_s)^2}{\Delta H_k}\left(1+\frac{\sqrt{\pi}}{2}+\frac{2}{\pi}\ln\frac{(2\sqrt{\pi})R_p}{4S}\right)^2\times\frac{(2R_p)^2S^2}{(2R)^4}\left(\frac{\bar{m}_r}{m_r(0)}\right)^2 N_{\text{pits}}$$

$$=\left(\frac{4\pi M_s}{1750}\right)^2\left(\frac{0.2}{\Delta H_k}\right)\times\frac{\{1+\frac{1}{2}\sqrt{\pi}+(2/\pi)\ln[(2\sqrt{\pi})R_p/4S]\}^2}{6.2937}\times\left(\frac{2R_p}{6\mu}\right)^2\left(\frac{S}{1\mu}\right)^2\left(\frac{20\text{ mil}}{2R}\right)^4\left(\frac{\bar{m}_r}{m_r(0)}\right)^2\times\left(\frac{N_{\text{pits}}}{1}\right)\times 43.5\text{ mOe},\quad(36)$$

(where 20 mil$=5\times10^2\,\mu$) for scattering out of the main resonance mode into modes with $k_z=0$ by N_{pits} pits with $2R_p\gg S$. The corresponding result for $2R_p=(2/\sqrt{\pi})S$ is obtained directly from (34). Replacing the bracket by 1 and $(2R_p)^2$ by $(4/\pi)S^2$ in (36) gives

$$H_1=\left(\frac{4\pi M_s}{1750}\right)^2\left(\frac{0.2}{\Delta H_k}\right)\left(\frac{S}{1\mu}\right)^3\left(\frac{20\text{ mil}}{2R}\right)^4\times\left(\frac{\bar{m}_r}{m_r(0)}\right)^2\left(\frac{N_{\text{pits}}}{1}\right)\times 8.81\text{ mOe}\quad(37)$$

for $2R_p=(2/\sqrt{\pi})S$.

For scattering of the main-resonance mode into modes with $k_z>0$, F_k^2 is much smaller than the value given in (33). For modes with $n_z=2, 4, 6, \ldots$, which are odd in z, $F_k^2=0$ because h_r is odd in z. For scattering into modes with $n_z=3, 5, 7, \ldots$, we write the demagnetization field of the pit as $\mathbf{h}=\mathbf{h}_0+\delta\mathbf{h}$, where $\mathbf{h}_0$ is independent of z. From Eq. (26) with z' replaced by $z'-z$, it is easy to calculate the value of h_+ for several values of z and χ in the neighborhood of pit. [For example, for $\chi=\frac{1}{2}S$, $h_x\cong\alpha(2\pi m_r)$, where $\alpha=0.499$, 0.458, and 0.352 for $z=0$, $\frac{1}{4}S$, and $\frac{1}{2}S$, respectively.] In this way, it is easy to show that

$$h_x\cong(0.499\text{–}0.352)2\pi m_r\cos(\pi z/S),\quad\text{for } 0<\chi<\tfrac{1}{2}S$$
$$\cong 0,\quad\text{for } \tfrac{1}{2}S<\chi$$

is a fair approximation to h_x. With this value of h_x,

$$\mathcal{H}\cong-\int d\mathbf{r}h_x m$$
$$\cong 2(2\pi m_r)0.147L_p{}^2S\int_{-S/2}^{S/2}dz\cos\frac{\pi z}{S}m_0\cos\frac{(n_z-1)\pi z}{S}.$$

Evaluating the integral and using $L_p=\pi^{1/2}R_p$ gives, for $n_z=3, 5, 7, \ldots$,

$$|\mathcal{H}|=4(0.147)\pi^{1/2}m_r(p)m_k(p)R_pS^2\frac{1}{n_z(n_z-2)}.\quad(38)$$

Comparing (38) and (32) shows that $(F_{k_x,k_y,0})^2$ in (33) should be reduced by the factor

$$\frac{(4/\pi^2)(0.147)^2}{\{1+\frac{1}{2}\sqrt{\pi}+(2/\pi)\ln[(2\sqrt{\pi})R_p/4S]\}^2}\frac{1}{n_z^2(n_z-2)^2},\quad(39)$$

which is equal to 6.54×10^{-5} for $2R_p=50\,\mu$, $2R=20$ mil, and $S=1\,\mu$. Thus, the scattering of the main-resonance mode into exchange branches by large pits ($2R_p\gtrsim S$) is much weaker than the scattering into other magnetostatic modes.

Evaluation of Σ_k for large pits ($2R_p\gtrsim S$). The scattering of the main-resonance mode into modes on the higher branches gives values of ΔH which are very small, typically of the order of a few mOe or less, because the factor in (39) is small. Furthermore, there are no degenerate modes for small S in $\perp$ resonance. For very large pits the range in k_x-k_y space of the coupling is so short that the main-resonance mode is not coupled to the higher branches in parallel resonance. That is, there are no modes on these branches which satisfy $k_x<\pi/R_p$ and $k_y<\pi/R_p$. Thus, we calculate the scattering into the modes of the main branch only.

The linewidth ΔH as a function of the angle θ_m between $\mathbf{H}_i$ and the normal to the plane of the film ($\theta_m=0$ in perpendicular resonance) can be obtained by evaluating the sum in Σ_k in (35). From (4), the value of $\omega_k-\omega_r$ is

$$\omega_k-\omega_r=2\pi|\gamma|M_s\sin^2\theta_m-\omega_r+\pi|\gamma|M_sk_fS\times(\cos^2\theta_m-\cos^2\phi\sin^2\theta_m).\quad(40)$$

We use the δ-function limit (9) for G_k. From the well-known result

$$\delta(f(x))=\sum_{x_0}\frac{\delta(x-x_0)}{|df/dx|_{x_0}},$$

where the x_0's are the zeros of f, it follows that

$$\delta(\cos^2\phi-E^2)=\frac{\delta(\phi-\phi_0)}{2|\sin\phi_0\cos\phi_0|},\quad(41)$$

where $\cos^2\phi_0\equiv E^2$. With $\sin\phi_0=(1-E^2)^{1/2}$, $\cos\phi_0=E$, $\delta(ax)=|a|^{-1}\delta(x)$, and $\omega_k-\omega_k-\omega_r$ given by (40), we find

$$\delta(\omega_k-\omega_r)=[2\pi|\gamma|M_sSk_f\sin^2\theta_mE(1-E^2)^{1/2}]^{-1}\times\delta(\phi-\phi_0),\quad(42)$$

where

$$E=[\cot^2\theta_m-(2\cot^2\theta_m-1)\pi/\sqrt{2}k_fL]^{1/2}.\quad(43)$$

We have used (4) with $\cos^2\phi=\frac{1}{2}$ (since $k_{rx}=k_{ry}=\pi/L$)

for ω_r. Approximating the sums over k_x and k_y in (35) by an integral over k_f and approximating $\theta(\pi/R_p-k_x)\times\theta(\pi/R_p-k_y)$ by $\theta(\pi/R_p-k_f)$ and using (42) gives (with $L^2=\pi R^2$)

$$\Sigma_k=\frac{1}{4}\frac{\Delta H_k}{4\pi M_s}\frac{(2R)^2}{S}\frac{1}{\sin^2\theta_m}\int_0^{\pi/R_p}dk_f\frac{1}{E(1-E^2)^{1/2}}. \quad (44)$$

The integral extends only over real values of the integrand since

$$\int_0^1 d\phi\delta(\cos^2\phi-E^2)=0$$

for $E(1-E^2)^{1/2}$ complex.

The integral in (44) can be evaluated exactly, but the result is too complicated to interpret easily. We therefore consider the values of the integral at several key values of θ_m, from which the general form of ΔH as a function of θ_m is obtained.

For $\theta_m=\pi/2$ (parallel resonance), $\cot^2\theta_m=0$ and (43) gives $E=(\pi/\sqrt{2}k_fL)^{1/2}$. The factor $(1-E^2)^{1/2}$ in (44) should be replaced by 1 because the contribution to the integral from the region of k_f near $k_L\equiv\pi/\sqrt{2}L$ [where $(1-E^2)^{1/2}$ is large] is greatly overestimated by replacing the sum by an integral. That is, for the very small values of $k_f\cong k_L$ there are only a few widely spaced points in k space, and the sum should not be replaced by an integral. Thus, with $\int dk_f k_f^{1/2}=\frac{2}{3}(\pi/R_p)^{3/2}$, (44) gives

$$\Sigma_{k_{\rm II}}=\frac{\pi}{3}(2\pi)^{1/4}\frac{\Delta H_k}{4\pi M_s}\frac{(2R)^{5/2}}{S(2R_p)^{3/2}}. \quad (45)$$

With (35) this gives

$$\Delta H_{\rm II}=\tfrac{1}{3}(2\pi)^{1/4}\left(\frac{4}{\pi}\right)^4 4\pi M_s\left(1+\tfrac{1}{2}\sqrt{\pi}+\frac{2}{\pi}\ln\frac{(2\sqrt{\pi})R_p}{4S}\right)^2\times\frac{(2R_p)^{1/2}S}{(2R)^{3/2}}\left(\frac{\bar{m}_r}{m_r(0)}\right)^2 N_{\rm pits}, \quad (46)$$

which can be written as

$$\Delta H_{\rm II}=\left(\frac{4\pi M_s}{1750}\right)\frac{\{1+\frac{1}{2}\sqrt{\pi}+(2/\pi)\ln[(2\sqrt{\pi})R_p/4S]\}^2}{6.2937}\times\left(\frac{2R_p}{6\mu}\right)^{1/2}\left(\frac{S}{1\mu}\right)\left(\frac{20\text{ mil}}{2R}\right)^{3/2}\left(\frac{\bar{m}_r}{m_r(0)}\right)^2\times N_{\rm pits}\times 3.3\text{ Oe}. \quad (47)$$

From (37), the value of $\Delta H_{\rm II}$ for $2R_p=(2/\sqrt{\pi})S$ is

$$\Delta H_{\rm II}=\left(\frac{4\pi M_s}{1750}\right)\left(\frac{S}{1\mu}\right)^{3/2}\left(\frac{20\text{ mil}}{2R}\right)^{3/2}\left(\frac{\bar{m}_r}{m_r(0)}\right)^2\times N_{\rm pits}\times 0.23\text{ Oe}. \quad (48)$$

For $2\cot^2\theta_m-1=0$, i.e., $\theta_m\cong 54.7°$, (43) gives $E=\sqrt{\frac{1}{2}}$. With $\int dk_f[E\sqrt{(1-E^2)}]^{-1}=2\pi/R_p$, (44) gives

$$\Sigma_k=\tfrac{3}{4}(\Delta H_k/4\pi M_s)(2R)^2/S \quad \text{for } 2\cot^2\theta_m-1=0.$$

Comparing this result with (45) gives

$$\Delta H_{54.7°}=\frac{9}{2(2\pi)^{1/4}}\left(\frac{2R_p}{2R}\right)^{1/2}\Delta H_{\rm II}, \quad (49)$$

which can be written as

$$\Delta H_{54.7°}=0.309\left(\frac{2R_p}{6\mu}\right)^{1/2}\left(\frac{20\text{ mil}}{2R}\right)^{1/2}\Delta H_{\rm II}. \quad (50)$$

For $\theta_m=\pi/4$, (43) gives $E=[1-(\pi/\sqrt{2}k_fL]^{1/2}$ and $(1-E^2)^{1/2}=(\pi/\sqrt{2}k_fL)^{1/2}$. Thus, $E(1-E^2)^{1/2}$ has the same value as in parallel resonance. With $\sin^2\theta_m=\frac{1}{2}$, we obtain

$$\Delta H_{45°}=2\Delta H_{\rm II}. \quad (51)$$

For θ_m slightly less than $\pi/4$, (43) gives $\sqrt{(1-E^2)}\cong[(\pi/\sqrt{2}k_fL)-(\cot^2\theta_m-1)]^{1/2}$. Replacing E by 1 as before in (44) gives

$$\Sigma_k=\frac{1}{4}\frac{\Delta H_k}{4\pi M_s}\frac{(2R)^2}{S}\frac{1}{\sin^2\theta_m}\times\int_0^{k_{ls}}dk_f\left(\frac{\pi}{\sqrt{2}k_fL}-(\cot^2\theta_m-1)\right)^{-1}, \quad (52)$$

where k_{ls} is the lesser of π/R_p and $\pi/\sqrt{2}L(\cot^2\theta_m-1)$. The integral has a maximum

$$\Sigma_{k\,\max}=\frac{\pi^2}{2}(2\pi)^{1/4}\frac{\Delta H_k}{4\pi M_s}\frac{(2R)^{5/2}}{S(2R_p)^{3/2}}$$

at the value of θ_m which makes

$$\pi/R_p=\pi/\sqrt{2}L(\cot^2\theta_m-1).$$

Comparing this result with (45) gives

$$\Delta H_{\max}=4.7\Delta H_{\rm II}. \quad (53)$$

For smaller values of θ_m (less than that at the peak), the δ-function approximation (9) becomes less accurate because the spacing is large for the modes with small values of k_f, and the integral in (44) gives values of Σ_k which are too large. In fact,

$$\Delta H\ll\Delta H_{\rm II} \quad \text{for } \theta_m \text{ near zero}. \quad (54)$$

This result, which can be proved by using (40), can be understood intuitively as follows: In perpendicular resonance there are no main-branch modes degenerate with the main-resonance mode, as seen in Fig. 1. As θ_m is increased from zero, it is intuitively clear that the

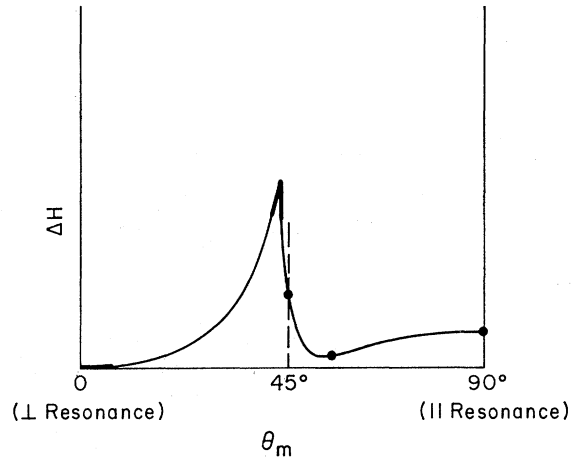

FIG. 5. Angular dependence of the two-magnon ΔH for scattering centers larger than the film thickness. The dots and heavy portions of the curve correspond to the explicit calculations given in the text.

density of degenerate main-branch modes does not increase suddenly to a large value.

The results (46), (50), (51), (53), and (54) are illustrated schematically in Fig. 5. The sharp peak at θ_m slightly less than 45° will be rounded off in practice. Since the angle α between the film normal and $\mathbf{H}_{\rm app}$ is less than θ_m, the peak in ΔH as a function of α will be at an angle considerably smaller than 45° in general. The ratio of $\Delta H_{\rm max}$ to $\Delta H_{\rm II}$ is independent of the pit radius R_p [see Eq. (53)], but the value of ΔH at the minimum between $\theta_m=45°$ and $\theta_m=90°$ is a function of R_p [see Eq. (50)]. These results for scattering by large pits are quite different from those for scattering by small pits, as seen by comparing Figs. 3 and 5.

It should be mentioned that it is possible that there may be an increase in the linewidth at the depinning angle as the angle is increased from the perpendicular-resonance side. If the mode is Portis pinned, then in perpendicular resonance m does not extend across the full thickness of the sample. At the depinning angle m should extend across the sample thickness, thereby sampling a larger region of the film. If this larger region is more inhomogeneous than the small one the linewidth should increase. As the angle is increased toward parallel resonance, the linewidth could either increase or decrease, depending on the nature of the inhomogeneities.

Finally, the factor $\partial H/\partial\omega$ in the relation

$$\Delta H=\frac{\partial H}{\partial\omega}\Delta\omega$$

can introduce some structure in the angular dependence of the linewidth. In YIG, with its small value of $4\pi M_s$, at X band this is a small factor.

4. TABLE OF THEORETICAL RESULTS

The following symbols are used in the results listed below: $2R$ is the film diameter; $2R_p$ is the pit diameter; S is the film thickness; m_r is the transverse (microwave) magnetization of the main-resonance mode; $m_r(0)$ is the maximum value of $m_r(\mathbf{r})$ (at $\mathbf{r}=0$); $\bar{m}_r$ is the value of m_r at a pit, averaged over all pits. For one pit in the center of the film $\bar{m}_r/m_r(0)=1$; $N_{\rm pits}$ is the number of pits.

See Fig. 2 for the following:

$$u_k^2\equiv\cos^2\theta_k=\frac{H_i+Dk^2+2\pi M_s-(\omega_r/|\gamma|)}{2\pi M_s},$$

$$u_0\equiv u_k|_{k=0},\quad u_s\equiv u_k|_{k=k_s},\quad k_{\rm max}\equiv(2\pi/\Lambda)^{1/2},$$

$$k_c\equiv\left(\frac{9}{2\pi^2}\right)^{1/3}\frac{\pi}{R_p}=0.769\frac{\pi}{R_p},\quad k_{{\rm max}\,r}\equiv\left(\frac{2\pi}{\Lambda}(1-u_0^2)\right)^{1/2},$$

$$k_d=\left(\frac{2\pi}{\Lambda}\right)^{1/2}u_0=u_0\frac{568\text{ Å}}{\sqrt{\Lambda}}4.4\times10^5\text{ cm}^{-1},$$

$$k_s\equiv\text{lesser of }(k_c,k_{{\rm max}\,r}).$$

The central results of the paper are the following:

(A) *Small pits* ($2R_p\ll S$). See Fig. 3.

For $k_c\ll k_{\rm max}$ and $k_c<k_{{\rm max}\,r}$

$$\Delta H_{\rm sml\ pits}=\left(\frac{4\pi M_s}{1750}\right)\left(\frac{2R_p}{0.25\mu}\right)\left(\frac{1\mu}{S}\right)\times\frac{(3u_s^2-1)^2+1.6}{5.6u_0}B\times27.2\text{ Oe} \tag{18a}$$

$$B=1,\qquad\text{for } k_d^2\gg k_s^2$$

$$=\frac{3}{2}\frac{1}{k_c}\left(\frac{2\pi}{\Lambda}\right)^{1/2}u_0,\quad\text{for } k_s^2\gg k_d^2.$$

For $k_c>k_{{\rm max}\,r}$,

$$\Delta H_{\rm vy\ sml\ pits}=\frac{5.6}{288}\left(\frac{2}{\pi}\right)^7 4\pi M_s\times\frac{(3u_s^2-1)^2+1.6}{5.6}\frac{(2R_p)^4}{S}B_s, \tag{18b}$$

$$B_s=k_{{\rm max}\,r}^3,\qquad\text{for}\quad Dk_{{\rm max}\,r}^2\ll2\pi M_s$$

$$=(2\pi/\Lambda)k_{{\rm max}\,r},\quad\text{for}\quad|k_d^2|\ll k_{\rm max}^2.$$

(B) *Large pits* ($2R_p\gtrsim S$). See Fig. 5.

(a) Parallel resonance

(1) $2R_p \gg S$

$$\Delta H_{\perp\perp}=\left(\frac{4\pi M_s}{1750}\right)\frac{\{1+\frac{1}{2}\sqrt{\pi}+(2/\pi)\ln[(2\sqrt{\pi})R_p/4S]^2}{6.2937}\times\left(\frac{2R_p}{6\mu}\right)^{1/2}\left(\frac{S}{1\mu}\right)\left(\frac{20\text{ mil}}{2R}\right)^{3/2}\left(\frac{\bar{m}_r}{m_r(0)}\right)^2 N_{\text{pits}}\times 3.3\text{ Oe}. \quad (47)$$

(2) $2R_p=(2/\sqrt{\pi})S$

$$\Delta H_{\perp\perp}=\left(\frac{4\pi M_s}{1750}\right)\left(\frac{S}{1\mu}\right)^{3/2}\left(\frac{20\text{ mil}}{2R}\right)^{3/2}\left(\frac{\bar{m}_r}{m_r(0)}\right)^2\times N_{\text{pits}}\times 0.23\text{ Oe}. \quad (48)$$

In the following results (b)–(e), $\Delta H_{\perp\perp}$ is given by (47) or (48), depending on the size of $2R_p/S$.

(b) Intermediate angle; $\theta_m=54.7°$

$$\Delta H_{54.7°}=0.309\left(\frac{2R_p}{6\mu}\right)^{1/2}\left(\frac{20\text{ mil}}{2R}\right)^{1/2}\Delta H_{\perp\perp}. \quad (50)$$

(c) Intermediate angle; $\theta_m=45°$

$$\Delta H_{45°}\cong 2\Delta H_{\perp\perp}. \quad (51)$$

(d) Angle for maximum ΔH;

$$\theta_m\cong\tan^{-1}\left[1-\frac{1}{4}\left(\sqrt{\frac{2}{\pi}}\right)\frac{2R_p}{2R}\right]$$

$$\Delta H_{\max}\cong 5\Delta H_{\perp\perp}. \quad (53)$$

(e) Small values of θ_m (near perpendicular resonance)

$$\Delta H_{\perp}\ll\Delta H_{\perp\perp}. \quad (54)$$

(*C*) *Perpendicular resonance in very thin films* (*higher branches above main-resonance mode*).

$$\Delta H_{\perp vt}\cong\left(\frac{\Delta H_k}{0.2}\right)\left(\frac{4\pi M_s}{1750}\right)\left(\frac{2R_p}{0.25\mu}\right)^3\times\left(\frac{4.5\times10^{-9}\text{ Oe cm}^2}{D}\right)\left(\frac{1\mu}{S}\right)\times 15.4\text{ mOe}. \quad (22)$$

Note: For parallel resonance and other values of θ_m not too close to zero (so that there are many exchange branches having modes with $\omega<\omega_{kr}$), Eq. (18a) is valid for very thin films.

(*D*) *Linewidths of higher-branch exchange modes.* The dependence of the linewidths of the exchange modes on the mode number n, where $k_{nz}=n\pi/S$, and on M_s is rather complicated. For small n, $\Delta H\sim 4\pi M_s n^3$; for intermediate n, ΔH can be proportional to $4\pi M_s n^2$ or to $(4\pi M_s)^2 n$; and for large n, $\Delta H\sim(4\pi M_s)^2 n^0$. The values of n at which the transitions between the different regions occur depend on the values of S, R_p, M_s, D, and H_i in a rather complicated way, as discussed briefly in the Appendix.

APPENDIX: EXCHANGE MODES IN PERPENDICULAR RESONANCE

The higher-branch exchange modes excited in the usual ferromagnetic-resonance experiments in thin films in perpendicular resonance have $\sin^2\theta_k\cong 0$. The dispersion relation for these modes is

$$\bar{\omega}=H_i+Dk_z^2,$$

as illustrated schematically by the dots in Fig. 2. Thus, in addition to the difference in the dispersion relations for thin films and bulk-type samples, the exchange modes are on the high-k edge of the manifold, while the main-resonance mode is near the $k=0$ edge. The density of degenerate states into which the excited mode scatters, therefore, is different for these two cases unless k_c is so large ($k_c>k_{\max r}$) that both modes scatter into all degenerate modes. Otherwise the k^2 factor in the density of states is larger for the exchange mode than for the main-resonance mode, making ΔH larger for the exchange mode.

It is assumed that the leading terms in the scattering Hamiltonian for scattering out of these exchange modes with $\mathbf{k}\neq 0$ can be approximated by (5) with the cutoff factor C_k replaced by

$$C_{k_{nk}}=1, \quad \text{for} \quad k_{nz}-k_z<k_c \quad \text{and} \quad k_f<k_c$$
$$=0, \quad \text{otherwise} \quad (A1)$$

where n denotes the relaxing exchange mode (having $k_{nz}=\pi n/S$ and $k_{nf}\cong 0$). The evaluation of the sum in (10) is fairly straightforward, but tedious. Since the general results would be quite cumbersome, the central features of the results and order-of-magnitude expressions for ΔH for three values of R_p and S will be given.

The nth exchange line consists of the lowest $-k_f$ mode on the nth branch plus small amounts of the larger $-k_f$ modes. Thus, the linewidth of the nth line is essentially determined by the loss of the lowest $-k_f$ mode on the nth branch. See Fig. 1. This mode scatters into the other modes on the same branch and to the degenerate modes on the lower branches, i.e., the branches having $k_z<k_{nz}$. Since the number of modes on a given branch which have $\omega_n-\Delta H<\omega<\omega_n+\Delta H$ is large, the sum over k_f can be replaced by an integral, and the sum on $\mathbf{k}$ becomes

$$\sum_k\rightarrow\sum_{k_z=k_{nz}-k_c}^{k_{nz}}\frac{\pi R^2}{\pi^2}\frac{\pi}{2}\int_0^{k_c}dk_f\,k_f. \quad (A2)$$

The factor $\pi R^2/\pi^2$ is from the density of states and the factor of $\frac{1}{2}\pi$ is from the integral of the azimuthal angle

over one quadrant (i.e., over positive k_x and k_y). If $k_{nz}-k_c$ is negative, the sum over k_z extends over all lower branches.

For a sufficiently large value n_{co} of n, the spacing along the k_f axis between the relaxing mode n (with $k_f\cong 0$) and the intercept of the next lower branch $(n-1)$ with the line $\omega=\omega_n$ is larger than the cutoff value k_c. In this case mode n cannot scatter into the other branches, and there is only intrabranch scattering into the modes with the same value of n and different values of k_f. The value of n_{co} is determined by equating $\bar{\omega}_{n_{co}}\equiv\omega_{n_{co}}/|\gamma|\cong H_i+D(n_{co}\pi/S)^2$ to

$$\bar{\omega}_{n_{co}-1}=H_i+D[(n_{co}-1)\pi/S]^2+\mathfrak{D}k_f^2, \qquad \text{(A3)}$$

where

$$\mathfrak{D}\equiv D+(2\pi M_s/k_z^2), \qquad \text{(A4)}$$

and setting $k_f=k_c\cong\pi/R_p$ in (A3) and $k_z=(n_{co}-1)\pi/S$ in (A4). Assuming that $n_{co}\gg 1$, this gives

$$n_{co}=\frac{1}{2}\left[\frac{\mathfrak{D}}{D}\left(\frac{S}{R_p}\right)^2-1\right]. \qquad \text{(A5)}$$

In (A3) and (A4), $\sin^2\theta_k=k_f^2/(k_f^2+k_z^2)$ has been approximated by k_f^2/k_z^2. Since $k_f=\pi/R_p$ here, this approximation is valid when

$$n_{co}\gg(S/R_p)^{1/2}, \qquad \text{(A6a)}$$

which is usually satisfied.

Since $\mathfrak{D}$ in (A4) is a function of $k_z=(n_{co}-1)\pi/S$, (A5) must be solved self-consistently. For $D(n_{co}\pi/S)^2\gg 2\pi M_s$,

$$n_{co}\cong\tfrac{1}{2}[(S/R_p)^2-1]; \qquad \text{(A6b)}$$

and for $D(n_{co}\pi/S)^2\ll 2\pi M_s$,

$$n_{co}\cong\left[\frac{1}{4}\frac{4\pi M_s}{D(\pi/S)^2}\left(\frac{S}{R_p}\right)^2\right]^{1/3}. \qquad \text{(A6c)}$$

The value of ΔH for this intrabranch scattering will now be calculated. From $\bar{\omega}_n=H_i+D(n\pi/S)^2$ and $\omega_k=H_i+D(n\pi/S)^2+\mathfrak{D}k_f^2$, the value of $\bar{\omega}_k-\bar{\omega}_r$ is

$$\bar{\omega}_k-\bar{\omega}_r=\mathfrak{D}k_f^2,$$

and $\sum_k$ in (10) becomes

$$\sum_k=\frac{\pi R^2}{\pi^2}\frac{\pi}{2}\int_0^\infty dk_f\, k_f\frac{(\frac{1}{2}\Delta H_k)^2}{(\mathfrak{D}k_f^2)^2+(\frac{1}{2}\Delta H)^2},$$

where the first term in the sum on k_z in (A2) was retained and the upper limit k_c of the integral was replaced by infinity since the integrand is small for $k_f\geqq k_c$. Evaluating the integral gives

$$\sum_k=\frac{\pi R^2}{16}\frac{\Delta H}{\mathfrak{D}}, \qquad \text{(A7)}$$

for the intrabranch scattering, and (10) gives

$$\Delta H=\frac{5.6}{9}\frac{4}{\pi^4}4\pi M_s\left[\frac{2R_p}{S}\right]^4 fU$$

$$=\left[\frac{4\pi M_s}{10^4}\right]\left[\frac{0.5}{S/2R_p}\right]^4 fU\times 16\text{ Oe}, \qquad \text{(A8)}$$

where

$$U=n^2, \quad \text{for } Dk_{nz}^2\ll 2\pi M_s$$

$$=2\pi M_s/D(\pi/S)^2, \quad \text{for } Dk_{nz}^2\gg 2\pi M_s$$

for $n>n_{co}$. Here a factor of f has been included to allow for the fact that the surface pits may not be closely packed on the surfaces of the film. For close packing, $f=1$, and for spacing between the pits, $f<1$. The crystallites in metallic films tend to extend across the full thickness of the films. A rounding of the crystallite edges by oxidation could give rise to surface pits. If the diameter d of the crystallites is less than S, then f should be of the order of unity. But if $d\geqq S$, then $f<1$, and if $d\gg S$, then $f\ll 1$. For the case of $f\cong 1$ and $Dk_{nz}^2\ll 2\pi M_s$, (A8) gives $\Delta H\cong 16n^2$ Oe for the present example, which is to be compared with $Dk_{nz}^2=8.6n^2$ Oe. Even though the perturbation is so large that the perturbation analysis is not valid for this case when $f\cong 1$, the result does indicate that the linewidth should be larger.

Consider the case of $S=4R_p=5000$ Å, $D=2.2\times 10^{-9}$ Oe cm^2, $D(\pi/S)^2=8.6$ Oe, and $4\pi M_s=10^4$ Oe. Equation (A6c) gives $n_{co}=17$. Since only odd modes usually have large intensities, all modes above the eight intense ones scatter strongly into only the modes on the same branch. The value of ΔH for these modes with $n>n_{co}$ is given by (A8).

Next consider the case of $S=20$ $R_p=5000$ Å, with the same values of D and M_s used above. The value of n_{co} is ~ 200, which is so large that the region in which ΔH is independent of k_{nz} is at values of n greater than any observed to date. For values of $k_{nz}\lesssim\pi/R_p$, i.e., $n\lesssim S/R_p=20$, mode n can scatter into all degenerate modes. The sum over k_z in (A2) then contains many terms, and the sum can be replaced by an integral over all degenerate states; thus, the result (18b) is valid for the modes with $n<20$. The value of Dk_{nz}^2 for the last of these modes, with $n=20$, is $\sim 2/3(2\pi M_s)$. For larger values of n, the integral does not extend over all degenerate states, and the value of ΔH is less than the value given in (18b).

For $S=8R_p=5000$ Å and the same values of D and M_s, it can be shown that $\Delta H\sim 4\pi M_s n^2$ for a small range of n around $n\cong 15$. The mode n scatters only into modes nearby in $\mathbf{k}$ space in this case, and the factor $n^2\sim k_n^2$ is the usual density-of-states factor.

In order to determine if the present model is valid, it would be necessary to inspect the film to determine the size $2R_p$ of the scattering centers and the packing factor f. In the absence of this information, it can be stated only that the results afford a possible explanation of several experimental results. For example, Phillips and Rosenberg[14] and Wigen[15] have reported $\Delta H\sim n^2$ for modes with $11\leqq n\leqq 21$ in a Co film and for $\sim 4\leqq n\leqq 9$ in a permalloy film, respectively. Two of the cases above give $\Delta H\sim n^2$ with the correct order of magnitude ($\Delta H\sim 100$ Oe for the large-n modes). Weber, Tannenwald, and Bajorek[16] have observed linewidths independent of n for large values of n ($9\leqq n\leqq n_{\max}$, where $n_{\max}$ ranged from 15 to 31). For $n=9$, the value of Dk_{nz}^2 is ~ 1600 Oe, which is considerably smaller than $2\pi M_s=5500$ Oe. Although the present results predict that ΔH is independent of n for large n, they cannot explain the fact that ΔH is independent of n for the smaller values of n.

[14] T. G. Phillips and H. M. Rosenberg, Phys. Letters **8**, 298 (1964).

[15] P. E. Wigen, Phys. Rev. **133**, A1557 (1964).

[16] R. Webber, P. E. Tannenwald, and C. Bajorek (unpublished).

PHYSICAL REVIEW B VOLUME 1, NUMBER 9 1 MAY 1970

Ferromagnetic Resonance in Thin Films. III. Theory of Mode Intensities

M. SPARKS*

Science Center, North American Rockwell Corporation, Thousand Oaks, California 91360

(Received 18 August 1969)

A theory of surface-spin pinning and its effects on the ferromagnetic-resonance mode intensities is presented. The pinning by a surface inhomogeneity (e.g., a demagnetization field from surface imperfections or an inhomogeneous saturation magnetization) of thickness ϵ is considered. Roughly speaking, the modes are nearly unpinned for a thin-surface inhomogeneity ($\epsilon^2\ll\Lambda/\pi$, where Λ is the exchange constant in the exchange field $\Lambda\nabla^2\mathbf{M}$), while the low-order modes are pinned by a thick-surface inhomogeneity ($\epsilon^2\ll\Lambda/\pi$ *not* satisfied). The theory indicates that the low-order modes should be pinned unless great care is exercied in the film preparation. In 80% Ni–20% Fe permalloy, $(\Lambda/\pi)^{1/2}\cong 90$ Å; thus, the surface region would have to be only a few lattice constants thick in order for there to be no pinning. These results are obtained by considering the equation of motion of the magnetization in the surface region as well as the bulk region. The intensities and frequencies of magnetostatic modes (negligible exchange energy) are relatively independent of surface-spin pinning, in contrast to the result for exchange modes (negligible microwave demagnetization energy) that pinning the surface spins gives rise to large intensities of even modes.

I. INTRODUCTION

SINCE Kittel's suggestion[1] in 1958 that the exchange integral in ferromagnetic materials could be obtained by ferromagnetic-resonance measurements in thin films, interest in this field has increased steadily.[1–5] Interpretation of experimental results has been obscured by a lack of understanding of the boundary conditions[6] at the film surfaces. The theories of Wigen, Kooi, and co-workers[4] (saturation magnetization M_z of surface layer different from that of the bulk) and Portis[3] (parabolic M_z) explain the positions and critical-angle depinning, but not the intensities, of exchange modes.[6a] Rado and Weertman[2] have shown that in the absence of a specific mechanism to pin[6] the surface spins, the exchange interaction makes the normal derivative of the magnetization zero for the long-wavelength modes. Thus, the intensities of all long-wavelength modes except the main-branch modes[6a] are zero in this case.

* Present address: The RAND Corp., Santa Monica, Calif.

[1] C. Kittel, Phys. Rev. **110**, 1295 (1958); C. F. Kooi, Phys. Rev. Letters **20**, 450 (1968); G. I. Lykken, *ibid.* **19**, 1431 (1967); T. G. Phillips, Proc. Roy. Soc. (London), **A292**, 224 (1966); R. F. Soohoo, *Magnetic Thin Films* (Harper and Row, New York, 1965); R. Weber and P. E. Tannenwald, Phys. Rev. **140**, A498 (1965); P. Pincus, *ibid.* **118**, 658 (1960); M. H. Seavey, Jr., and P. E. Tannenwald, Phys. Rev. Letters, **1**, 168 (1958); H. S. Jarrett and R. K. Waring, Phys. Rev. **111**, 1223 (1958); Z. Frait and M. Ondris, Czech. J. Phys. **B11**, 463 (1961); L. Néel, J. Phys. Radium **15**, 15 (1954); M. Nisenoff and R. W. Terhune, J. Appl. Phys. **36**, 732 (1965).

[2] G. T. Rado and J. R. Weertman, J. Phys. Chem. Solids **11**, 315 (1959).

[3] A. M. Portis, Appl. Phys. Letters **2**, 69 (1963).

[4] C. F. Kooi, P. E. Wigen, M. R. Shanabarger, and J. V. Kerrigan, J. Appl. Phys. **35**, 791 (1964); P. E. Wigen, C. F. Kooi, and M. R. Shanabarger, *ibid.* **35**, 3302 (1964); E. Hirota, J. Phys. Soc. Japan **19**, 1 (1964).

[5] P. E. Wigen, C. F. Kooi, M. R. Shanabarger, and T. D. Rossing, Phys. Rev. Letters **9**, 206 (1962).

[6] The surface spins are said to be *pinned* (or *unpinned*) if the microwave magnetization $\mathbf{m}$ is zero [or $d\mathbf{m}/dz'=0$] at the surface. See the discussion of (1.4) in the text.

[6a] Exchange modes have negligible microwave demagnetization energy, and magnetostatic modes have negligible exchange energy. The main-branch modes have the smallest value of $k_{z'}$, where $\hat{z}'$ is the film normal.